GEQM: A QUALITY METRIC FOR GRAY-LEVEL EDGE MAPS BASED ON STRUCTURAL MATCHING

Won-Dong Jang[†] *Jae-Young Sim*[‡] *Chang-Su Kim*[†]

[†]School of Electrical Engineering, Korea University, Seoul, Korea
[‡]School of Electrical and Computer Engineering,
Ulsan National Institute of Science and Technology, Ulsan, Korea
E-mails: wdjang@mcl.korea.ac.kr, jysim@unist.ac.kr, cskim@mcl.korea.ac.kr

ABSTRACT

An accurate quality metric, called GEQM, for gray-level edge maps based on the structural matching of edge pixels is proposed in this work. We design the positional matching cost, which reflects the distance between two edge pixels, and the structural matching cost, which measures the structural shapes of edges as well as the differences of edge strength levels. Based on the cost functions, we perform the graph-cut optimization to obtain the optimal pixel-based matching between source and target edge maps bidirectionally. Finally, we compute the GEQM score by summing up the optimal matching costs of all edge pixels. Experimental results show that the proposed GEQM performs the edge map quality assessment more accurately and more reliably than conventional metrics. Especially, GEQM is suitable for assessing the qualities of synthesized intermediate views in multi-view image processing.

Index Terms— Image quality assessment, edge map quality assessment, gray-level edge map, structural matching, and multi-view image processing.

1. INTRODUCTION

The peak signal-to-noise ratio (PSNR) is one of the most widely employed image quality measures, which is based on the mean squared error of pixel values between two images. PSNR, however, does not reflect the characteristics of human visual system (HVS) faithfully. Several alternative measures have been proposed based on HVS. Wang *et al*. [1] proposed the structural similarity (SSIM), which combines the luminance, contrast, and structure terms. Sheikh and Bovik [2] presented the visual information fidelity, which quantifies the similarity between an original image and its distorted version using the mutual information. Recently, Liu *et al*. [3] proposed an image quality measure based on the gradient similarity (GSM).

Edges in an image represent object boundary information, and their distortions are more noticeable to HVS than the distortions in smooth regions. This means that the subjective quality of an image can be assessed by investigating the distortions in its edge map. More specifically, given an image and its distorted version, we can extract the respective edge maps. Then, we can compute the similarity between the two edge maps to assess the quality of the distorted image. However, it is not trivial to measure the similarity between the edge maps, since the distorted edge map may generate false edges and remove or displace true edges.

The general image quality measures in [1–3] are inappropriate for assessing edge map qualities. Several edge map quality metrics have been specially designed based on pixel matching. Pratt [4] proposed the figure of merit (FOM), which matches detected edges to ground-truth edges based on the closest distance criterion. Bowyer *et al*. [5] also proposed the closest distance metric (CDM) for edge map quality assessment. While FOM performs many-to-one matching of pixels and is applicable to binary edge maps only, CDM enforces one-to-one matching and can assess the qualities of gray-level edge maps as well. Prieto and Allen [6] formulated the pixel correspondence metric (PCM), which matches gray-level edges based on the positional difference and the edge intensity difference criteria. These quality metrics, however, do not consider the structural similarity between edge maps and may yield incorrect assessment results. Jang and Kim [7] proposed the structural edge quality metric (SEQM) by taking into account the structural similarity, but it can be applied to binary edge maps only.

In this work, we propose a novel quality metric for gray-level edge maps, called gray-level edge quality metric (GEQM), which matches the structures of edge pixels between source and target edge maps. We design the positional matching cost that reflects the distance between two corresponding edge pixels. We also design the structural matching cost that measures the structural shapes of edges and the differences of edge strength levels. Then, we find the optimal matching for each edge pixel using the graph-cut optimization [8]. Finally, we compute the GEQM score by summing up the matching costs for all edge pixels bidirectionally. Experimental results show that the proposed GEQM assesses the qualities of gray-level edge maps more accurately and more reliably than the conventional metrics [1, 3, 5, 6]. Furthermore, it is demonstrated that GEQM is suitable for assessing the qualities of synthesized intermediate views in multi-view image processing.

The rest of this paper is organized as follows. Section 2 describes the proposed GEQM, Section 3 presents experimental results, and Section 4 concludes this work.

2. GRAY-LEVEL EDGE QUALITY METRIC

We regard a pixel, which has a gradient magnitude larger than a threshold, as an edge pixel. Let $\mathcal{S} = \{\mathbf{s}_1, \mathbf{s}_2, ..., \mathbf{s}_M\}$ and $\mathcal{T} = \{\mathbf{t}_1, \mathbf{t}_2, ..., \mathbf{t}_N\}$ denote the sets of edge pixels in a source edge map I_s and a target edge map I_t, respectively, where M and N are the numbers of edge pixels. We find the matching from $\mathcal{S}$ to $\mathcal{T}$. For

This work was supported partly by the National Research Foundation of Korea(NRF) grant funded by the Ministry of Science, ICT & Future Planning (MSIP) (No. 2009-0083495), and partly by the Global Frontier R&D Program on Human-centered Interaction for Coexistence funded by the National Research Foundation of Korea grant funded by the Korean Government (MSIP) (2011-0031648)

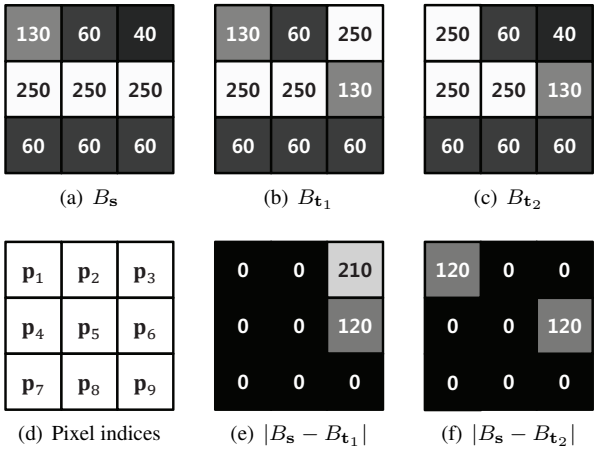

(a) $B_{\mathbf{s}}$ (b) $B_{\mathbf{t}_1}$ (c) $B_{\mathbf{t}_2}$

(d) Pixel indices (e) $|B_{\mathbf{s}} - B_{\mathbf{t}_1}|$ (f) $|B_{\mathbf{s}} - B_{\mathbf{t}_2}|$

Fig. 1. Structural similarity and SAD: (a) source block $B_{\mathbf{s}}$, (b) target block $B_{\mathbf{t}_1}$, (c) target block $B_{\mathbf{t}_2}$, (d) pixel indices, (e) difference block $|B_{\mathbf{s}} - B_{\mathbf{t}_1}|$, and (f) difference block $|B_{\mathbf{s}} - B_{\mathbf{t}_2}|$. The numbers denote gray-levels or their absolute differences.

each edge pixel $\mathbf{s} \in \mathcal{S}$ in the source map, we search the candidate edge pixels $\mathbf{t}$'s in the target map, which are within the 5×5 window centered at the position of $\mathbf{s}$. In general, different edge maps have different numbers of edge pixels. Therefore, the proposed GEQM allows many-to-one matching of edge pixels.

2.1. Matching Cost Design

First, we use the positional matching cost $C_{\text{pos}}(\mathbf{s}, \mathbf{t})$ to measure the Euclidean distance between $\mathbf{s}$ and $\mathbf{t}$.

$$C_{\text{pos}}(\mathbf{s}, \mathbf{t}) = \frac{1}{R}\sqrt{(x(\mathbf{s}) - x(\mathbf{t}))^2 + (y(\mathbf{s}) - y(\mathbf{t}))^2}, \quad (1)$$

where $(x(\mathbf{s}), y(\mathbf{s}))$ and $(x(\mathbf{t}), y(\mathbf{t}))$ are the xy-coordinates of $\mathbf{s}$ and $\mathbf{t}$, respectively. R is a normalization constant, which adjusts the weight of the positional term in the total matching cost. We empirically set $R = 10$ in this work.

Next, we measure the similarity of edge patterns by comparing the sum of absolute differences (SAD) between the two 3×3 blocks, which are centered at $\mathbf{s}$ and $\mathbf{t}$, respectively. However, SAD may not reflect the structural similarity between the two blocks correctly. For example, Fig. 1(a) is a source block $B_{\mathbf{s}}$ at $\mathbf{s}$, and Figs. 1(b) and (c) are two candidate target blocks $B_{\mathbf{t}_1}$ and $B_{\mathbf{t}_2}$ at $\mathbf{t}_1$ and $\mathbf{t}_2$. Fig. 1(d) shows pixel indices within a block. Figs. 1(e) and (f) depict the absolute differences from $B_{\mathbf{s}}$ to $B_{\mathbf{t}_1}$ and $B_{\mathbf{t}_2}$, respectively. In Fig. 1(e), $\mathbf{p}_3$ and $\mathbf{p}_6$ are associated with relatively large differences of 210 and 120. On the other hand, in Fig. 1(f), both $\mathbf{p}_1$ and $\mathbf{p}_6$ have a difference of 120. Thus, the SAD values in Figs. 1(e) and (f) are 330 and 240, respectively. Therefore, if only the SAD feature is employed, $B_{\mathbf{t}_2}$ is declared to be more similar to $B_{\mathbf{s}}$ than $B_{\mathbf{t}_1}$ is. But $B_{\mathbf{t}_1}$ is structurally more similar to $B_{\mathbf{s}}$ than $B_{\mathbf{t}_2}$ is. This is because $\mathbf{p}_3$ and $\mathbf{p}_6$ are spatially closer to each other than $\mathbf{p}_1$ and $\mathbf{p}_6$ are.

Based on the above observations, before computing the structural matching cost, we locally match pixels in a source block $B_{\mathbf{s}}$ to those in a target block $B_{\mathbf{t}}$. We form a bipartite graph between nine pixels in $B_{\mathbf{s}}$ and those in $B_{\mathbf{t}}$, where link (m, n) connects $\mathbf{p}_m$ in $B_{\mathbf{s}}$ and $\mathbf{p}_n$ in $B_{\mathbf{t}}$. We assign weight $w_{\mathbf{s},\mathbf{t}}(m, n)$ to link (m, n) by

$$w_{\mathbf{s},\mathbf{t}}(m,n) = H(m,n) \times \left(1 - \frac{|B_{\mathbf{s}}(m) - B_{\mathbf{t}}(n)| + |B_{\mathbf{s}}(n) - B_{\mathbf{t}}(m)|}{2 \cdot 255}\right) \quad (2)$$

where $B(k)$ denotes the edge strength level at pixel position $\mathbf{p}_k$ in block B. $H(m, n)$ is a monotonically decreasing function of the l_1-distance between pixel positions $\mathbf{p}_m$ and $\mathbf{p}_n$. We set the values of $H(m, n)$ as 1, 0.8, and 0.5, when the associated l_1-distances are 0, 1, and 2, respectively, and set $H(m, n) = 0$ otherwise. Note that $0 \le w_{\mathbf{s},\mathbf{t}}(m, n) \le 1$. Also, $w_{\mathbf{s},\mathbf{t}}(m, n)$ becomes larger, when $\mathbf{p}_m$ and $\mathbf{p}_n$ are spatially closer to each other and they have more similar edge strength levels. In other words, a large $w_{\mathbf{s},\mathbf{t}}(m, n)$ indicates that $\mathbf{p}_m$ in $B_{\mathbf{s}}$ and $\mathbf{p}_n$ in $B_{\mathbf{t}}$ are good matching candidates.

Then, we find the optimal set $\mathcal{M}$ of the nine pairs (m, n)'s, which represents the one-to-one matching with the largest sum of the weights $w_{\mathbf{s},\mathbf{t}}(m, n)$'s. The Hungarian method [9] can be used to obtain the optimal solution exactly. However, we adopt a greedy approach to solve this combinatorial problem sub-optimally in an efficient way. We first select the matching pair (u, v) with the maximum weight and include it in $\mathcal{M}$. We then set all weights, associated with $\mathbf{p}_u$ in the source block and $\mathbf{p}_v$ in the target block, to be 0. Then, we select the matching pair of the next maximum weight, include it in $\mathcal{M}$, and set the associated weights to 0. We repeat this procedure, until we select all nine pairs. Moreover, we enforce that the center pixel $\mathbf{p}_5$ of the source block is matched to that of the target block, by setting all weights of $w_{\mathbf{s},\mathbf{t}}(5, n)$'s and $w_{\mathbf{s},\mathbf{t}}(m, 5)$'s to 0 except for $w_{\mathbf{s},\mathbf{t}}(5, 5)$.

Now we define the structural matching cost $C_{\text{str}}(\mathbf{s}, \mathbf{t})$ between $\mathbf{s}$ and $\mathbf{t}$ as

$$C_{\text{str}}(\mathbf{s}, \mathbf{t}) = \frac{\exp(\bar{w}(\mathbf{s}, \mathbf{t})/\sigma^2) - \exp(1/\sigma^2)}{1 - \exp(1/\sigma^2)}, \quad (3)$$

where $\bar{w}(\mathbf{s}, \mathbf{t})$ is the average weight of the nine pairs in the optimal set $\mathcal{M}$ and $\sigma^2 = 0.2$. As $\bar{w}(\mathbf{s}, \mathbf{t})$ decreases from 1 to 0, the structural matching cost $C_{\text{str}}(\mathbf{s}, \mathbf{t})$ increases from 0 to 1. The exponential operator in (3) is used to make the structural matching cost sensitive to variations of $\bar{w}(\mathbf{s}, \mathbf{t})$ near value 1.

Finally, we combine the positional cost $C_{\text{pos}}(\mathbf{s}, \mathbf{t})$ and the structural cost $C_{\text{str}}(\mathbf{s}, \mathbf{t})$ to compute the total matching cost

$$C_{\text{total}}(\mathbf{s}, \mathbf{t}) = 1 - (1 - C_{\text{pos}}(\mathbf{s}, \mathbf{t})) \times (1 - C_{\text{str}}(\mathbf{s}, \mathbf{t})). \quad (4)$$

It is worth to note that we do not take the simple multiplication of $C_{\text{pos}}(\mathbf{s}, \mathbf{t})$ and $C_{\text{str}}(\mathbf{s}, \mathbf{t})$ as a total cost. In such a case, if either $C_{\text{pos}}(\mathbf{s}, \mathbf{t})$ or $C_{\text{str}}(\mathbf{s}, \mathbf{t})$ is 0, the total cost becomes 0 regardless of the other cost. On the contrary, the proposed cost $C_{\text{total}}(\mathbf{s}, \mathbf{t})$ in (4) becomes 0 only if both $C_{\text{pos}}(\mathbf{s}, \mathbf{t})$ and $C_{\text{str}}(\mathbf{s}, \mathbf{t})$ are 0 simultaneously. Also, note that $0 \le C_{\text{total}}(\mathbf{s}, \mathbf{t}) \le 1$.

2.2. Global Optimization

Intuitively speaking, for each edge pixel $\mathbf{s}$ in the source map, we find the best matching edge pixel $\mathbf{t}$ in the target map by minimizing the total cost function $C_{\text{total}}(\mathbf{s}, \mathbf{t})$. However, as done in [7], we adopt a global optimization scheme to obtain more reliable results. We define an energy function $E(\mathbf{L})$ by integrating the data term and the smoothness term together, given by

$$E(\mathbf{L}) = \sum_{\mathbf{s}_i \in \mathcal{S}} C_{\text{total}}(\mathbf{s}_i, \mathbf{s}_i + \mathbf{l}_i) + \delta \cdot \sum_{\mathbf{s}_i \in \mathcal{S}} \sum_{\mathbf{s}_j \in \mathcal{N}_i} C_{\text{smooth}}(\mathbf{l}_i, \mathbf{l}_j) \quad (5)$$

Table 1. Gray-level edge map quality assessment results of PCM, CDM, GSM, SSIM, PSNR, and the proposed GEQM. GEQM scores are multiplied by 100. The scores marked with an asterisk denote that the quality assessment results are inconsistent with the noise intensities.

		Gaussian noises			Speckle noises			Salt-and-Pepper noises			Gaussian blur			JPEG compression		
Image	Measure	32.5	65.0	97.5	0.002	0.003	0.004	0.01	0.02	0.03	0.5	1.0	2.0	50	30	10
Baboon	PCM	96.51	95.53	94.21	97.88	97.67	97.17	96.64	94.43	91.82	95.92	89.29	88.26	94.55	93.34	91.44
	CDM	96.50	95.50	95.08	97.20*	96.53*	97.03*	98.49	96.79	93.24	94.84	88.59	85.71	94.60	92.32	71.46
	GSM	99.38	99.03	98.76	99.75	99.66	99.58	97.84*	95.71*	96.62*	99.41	97.24	96.05	98.88	98.57	97.67
	SSIM	85.29	75.16	67.34	94.93	92.78	90.79	75.33	57.15	49.16	90.09	43.85	25.85	70.21	60.41	37.49
	PSNR	30.11	27.06	25.30	34.93	33.10	31.88	20.47*	17.13*	20.16*	28.65	21.33	19.84	26.12	24.71	22.22
	GEQM	88.26	83.80	80.53	93.53	92.10	90.95	94.63	88.91	77.55	87.64	74.33	70.38	83.43	80.98	74.35
Barbara	PCM	92.68	91.94	90.89	95.95	95.06	95.02	96.42	93.65	91.54	96.52	93.23	91.36	94.18	94.01	93.65
	CDM	95.47	94.46	93.67	94.38*	95.30*	95.31*	98.26	96.34	89.87	92.11	78.00	76.53	87.28	80.41	58.70
	GSM	99.22	98.81	98.47	99.73	99.64	99.56	97.36*	94.81*	95.62*	99.65	98.23	97.03	99.20	98.91	98.03
	SSIM	75.93	64.49	57.26	93.00	90.61	88.42	72.95	52.22	47.85	93.94	69.59	54.74	80.63	74.97	57.98
	PSNR	29.79	26.70	24.99	34.59	32.83	31.55	19.44*	16.23*	19.08*	30.57	23.36	21.67	28.78	27.09	24.27
	GEQM	87.59	82.77	79.43	93.91	92.59	91.48	94.42	88.73	80.08	92.23	83.37	80.04	88.02	85.61	77.65
Lena	PCM	92.64	91.43	90.49	94.70	94.01	93.61	96.46	93.74	91.50	97.40	94.52	92.93	95.41*	95.42*	94.28*
	CDM	95.14	94.34	93.72	94.90*	94.84*	95.06*	98.06	96.23	89.97	89.67	70.66	68.29	75.55	64.16	49.34
	GSM	99.09	98.57	98.19	99.65	99.54	99.44	96.71*	94.05*	95.09*	99.76	98.58	97.57	99.30	99.03	98.01
	SSIM	70.01	57.57	50.14	88.49	84.69	81.34	65.92	47.34	44.56	96.33	75.80	62.27	84.36	78.70	59.29
	PSNR	29.47	26.28	24.53	34.36	32.50	31.13	19.14*	16.19*	19.19*	33.41	25.20	22.97	30.40	28.60	25.07
	GEQM	87.13	81.92	78.32	93.47	92.01	90.74	93.62	88.17	81.52	94.69	87.58	84.62	90.13	87.22	75.74
Peppers	PCM	92.72	92.07	90.69	95.83	95.12	94.81	96.48	93.45	92.18	97.39	94.21	92.62	95.50*	95.68*	95.08*
	CDM	94.87*	93.93*	94.48*	95.32*	94.31*	94.74*	98.18	96.21	90.45	91.36	74.71	73.20	80.25	72.32	57.36
	GSM	99.19	98.69	98.31	99.69	99.60	99.51	97.19*	94.41*	95.41*	99.78	98.49	97.26	99.05*	98.15*	98.17*
	SSIM	69.87	57.52	50.27	90.28	86.88	84.22	69.62	48.75	46.52	97.30	80.70	66.98	86.47	81.55	64.01
	PSNR	34.46	32.58	31.24	19.62*	16.11*	19.29*	30.76	28.99	25.60	29.75	26.55	24.69	30.76	28.99	25.60
	GEQM	87.48	82.41	78.75	93.73	92.32	91.18	94.31	88.67	82.20	94.97	87.66	84.36	90.26	87.49	78.17

where $\mathcal{N}_i$ denotes the 8-connected neighbor edge pixels of $\mathbf{s}_i$ and $\delta = 0.1$. $\mathbf{l}_i$ and $\mathbf{l}_j$ denote the matching vectors at $\mathbf{s}_i$ and $\mathbf{s}_j$, respectively, and $\mathbf{L}$ is the set of all $\mathbf{l}_i$'s. The smoothness cost $C_{\text{smooth}}(\mathbf{l}_i, \mathbf{l}_j)$ is defined as

$$C_{\text{smooth}}(\mathbf{l}_i, \mathbf{l}_j) = \begin{cases} 0, & \text{if } \mathbf{l}_i = \mathbf{l}_j, \\ 1, & \text{if } \mathbf{l}_i \neq \mathbf{l}_j. \end{cases} \tag{6}$$

We obtain the optimal $\mathbf{L}^*$ by minimizing $E(\mathbf{L})$ using the graph-cut algorithm [8].

2.3. GEQM Score Computation

We define the directional matching cost $C(I_s, I_t)$ from the source map I_s to the target map I_t as the sum of the total matching costs associated with the optimal matching vectors $\mathbf{l}_i^*$'s in $\mathbf{L}^*$.

$$C(I_s, I_t) = \sum_{\mathbf{s}_i \in \mathcal{S}} C_{\text{total}}(\mathbf{s}_i, \mathbf{s}_i + \mathbf{l}_i^*). \tag{7}$$

Since we allow many-to-one matching, both $C(I_s, I_t)$ and $C(I_t, I_s)$ should be considered together for more reliable quality assessment. We compute the GEQM score between I_s and I_t by

$$\text{GEQM}(I_s, I_t) = 1 - \frac{C(I_s, I_t) + C(I_t, I_s)}{|\mathcal{S}| + |\mathcal{T}|}, \tag{8}$$

where $|\mathcal{S}|$ and $|\mathcal{T}|$ are the numbers of edge pixels in I_s and I_t, respectively. Note that $0 \leq \text{GEQM}(I_s, I_t) \leq 1$. GEQM returns the highest score 1, when the two edges maps are identical. On the contrary, it returns a low score, when the edge maps are dissimilar from each other.

3. EXPERIMENTAL RESULTS

3.1. Quality Assessment of Gray-Level Edge Maps

We evaluate the performance of the proposed GEQM using four classical test images "Baboon," "Barbara," "Lena," and "Peppers." We first obtain the ground-truth gray-level edge maps by applying the first-order central difference gradient filter with coefficients $\{-1, 0, 1\}$ to the original images. Then, we extract the edge maps of distorted images and measure their similarities to the ground-truth edge maps. We test the following distortion models: additive zero-mean Gaussian noises with variances 32.5, 65.0, and 97.5, multiplicative speckle noises with variances 0.002, 0.003, and 0.004, salt-and-pepper noises with occurrence probabilities 0.01, 0.02, and 0.03, Gaussian blur filters of size 5×5 with variances 0.5, 1.0, and 2.0, and JPEG compression with quality factors 50, 30, and 10. We regard pixels, whose gradient magnitudes are larger than 0, as edge pixels.

We compare the edge map quality assessment results of the proposed GEQM with those of the conventional metrics PCM [6], CDM [5], GSM [3], SSIM [1], and PSNR. In PCM and CDM, the maximum matching distance is set to 2, as in the proposed GEQM. Table 1 shows the comparison results. In all measures, a higher score means that the two edge maps are more similar. Therefore, scores should decrease as noise intensities increase. But we observe that conventional metrics yield inconsistent results in some cases. Specifically, PCM assigns higher scores to the JPEG compressed images with lower quality factors on the "Lena" and "Peppers" images. Also, CDM fails to provide consistent results with noise intensities, in the cases of the Gaussian noises on "Peppers" and the speckle noises on all four images. GSM also fails for the salt-and-pepper noises on all images and the JPEG compression tests on "Peppers." PSNR fails for the speckle noises on "Peppers" and the salt-and-pepper noises on "Baboon," "Barbara," and "Lena." Notice that only SSIM and the proposed GEQM yield decreasing quality scores with increasing noise intensities in all tests.

3.2. Quality Assessment of 3D Intermediate Views

Next, we apply the proposed GEQM to measure the qualities of intermediate view frames, which are synthesized from multi-view images using stereo matching techniques. We use four datasets: "Poster" and "Venus" from the 2001 stereo datasets [10] and "Cones" and "Teddy" from the 2003 stereo datasets [11]. We take the 2nd and the 6th views as the left and the right images, respectively, and synthesize the 4th view as an intermediate view. Notice that the quality of a synthesized intermediate view depends

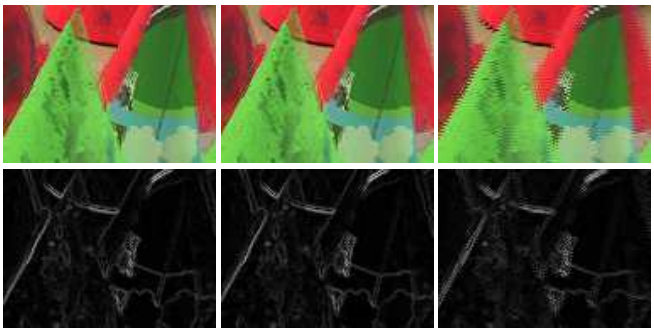

(a) (b) (c)

Fig. 2. Synthesized intermediate views (upper) and the corresponding edge maps (below) on the "Cones" dataset, which are obtained from (a) the ground-truth depth maps, (b) the depth maps with shift noises, and (c) the depth maps with swap noises, respectively.

mainly on the estimated depth maps of the left and the right images, and that noticeable distortions in the intermediate view generally occur near object boundaries. Thus, the proposed GEQM can assess the quality of an intermediate view faithfully by investigating its edge map.

We obtain the ground-truth edge map of the intermediate view using the ground-truth depth maps of the left and the right images. Then, we extract distorted edge maps of the intermediate view using noisy depth maps. We apply two kinds of noises to obtain the distorted depth maps [7]: the shift noise for shifting pixels to the left by one pixel, and the swap noise for moving pixels to the left or right by one pixel alternately.

Fig. 2 shows the noise effects on the intermediate view synthesis. We see that swap noises in Fig. 2(c) distorts the synthesized image more severely than shift noises in Fig. 2(b). Table 2 compares the edge map quality assessment results on synthesized intermediate views. PCM provides higher scores for swap noises than for shift noises on "Poster" and "Cones," which is contradictory to the observation in Fig. 2. CDM also exhibits inconsistent results on "Poster." SSIM and PSNR provides inconsistent results on all datasets. In contrast, the proposed GEQM properly returns higher scores for shift noises than for swap noises in all tests.

Table 2. Comparison of edge map quality assessment results for synthesized intermediate views. GEQM scores are multiplied by 100. The scores marked with an asterisk denote inconsistent assessment results.

Image	Measure	Shift	Swap
Poster	PCM	93.01*	93.16*
	CDM	88.87*	89.06*
	GSM	98.35*	98.79*
	SSIM	65.32*	66.96*
	PSNR	22.56*	23.11*
	GEQM	91.22	84.15
Venus	PCM	94.30	93.89
	CDM	90.06	89.71
	GSM	98.88*	99.18*
	SSIM	76.29*	77.78*
	PSNR	24.96*	25.52*
	GEQM	92.53	88.90
Cones	PCM	93.74*	94.16*
	CDM	91.87	91.44
	GSM	98.55*	98.91*
	SSIM	60.05*	61.76*
	PSNR	24.14*	24.74*
	GEQM	90.67	84.86
Teddy	PCM	94.85	94.69
	CDM	92.00	91.13
	GSM	98.98*	99.23*
	SSIM	74.01*	75.05*
	PSNR	25.64*	26.22*
	GEQM	92.30	88.95

4. CONCLUSIONS

We proposed an efficient gray-level edge quality metric, called GEQM, which takes the structural similarity and the positional similarity of edge maps into account. The proposed GEQM estimates the matching costs for possible pairs of edge pixels between two edge maps. Then, it minimizes the pixel-wise matching cost globally, using the graph-cut optimization technique, and determines the optimal matching pairs. Then, it employs the resulting optimal costs to compute the GEQM score. Simulation results demonstrated that GEQM provides more accurate and reliable quality assessment than the conventional metrics [1, 3, 5, 6]. Moreover, we verified that GEQM is a promising technique for assessing the qualities of synthesized intermediate views in multi-view image processing.

5. REFERENCES

[1] Z. Wang, A. C. Bovik, H. R. Sheikh, and E. P.Simoncelli, "Image quality assessment: From error visibility to structural similarity," *IEEE Trans. Image Process.*, vol. 13, no. 4, pp. 600–612, Apr. 2004.

[2] H. R. Sheikh and A. C. Bovik, "Image information and visual quality," *IEEE Trans. Image Process.*, vol. 15, no. 2, pp. 430–444, Feb. 2006.

[3] A. Liu, W. Lin, and M. Narwaria, "Image quality assessment based on gradient similarity," *IEEE Trans. Image Process.*, vol. 21, no. 4, pp. 1500–1512, Apr. 2012.

[4] W. K. Pratt, *Digital Image Processing*, New York: Wiley Interscience, 1978.

[5] K. Bowyer, C. Kranenburg, and S. Dougherty, "Edge detector evaluation using empirical ROC curves," *Comput. Vis. Image Understand.*, vol. 84, no. 1, pp. 77–103, June 2001.

[6] M. S. Prieto and A. R. Allen, "A similarity metric for edge images," *IEEE Trans. Pattern Anal. Mach. Intell.*, vol. 25, no. 10, pp. 1265–1273, Oct. 2003.

[7] W. D. Jang and C. S. Kim, "SEQM: Edge quality assessment based on structural pixel matching," Nov. 2012.

[8] Y. Boykov, O. Veksler, and R. Zabih, "Fast efficient approximate energy minimization via graph cuts," *IEEE Trans. Pattern Anal. Mach. Intell.*, vol. 20, no. 12, pp. 1222–1239, Nov. 2001.

[9] H. W. Kuhn, "The Hungarian method for the assignment problem," *Naval Res. Logist. Quart.*, vol. 2, no. 1, pp. 83–97, 1955.

[10] D. Scharstein and R. Szeliski, "A taxonomy and evaluation of dense two-frame stereo correspondence algorithms," *Int. J. Comput. Vis.*, vol. 47, pp. 7–42, Apr. 2002.

[11] D. Scharstein and R. Szeliski, "High-accuracy stereo depth maps using structured light," June 2003, vol. 1, pp. 195–202.